Real-Time Output Regulation of a Twin Rotor MIMO System

Jorge Álvarez * **Carlos Armenta** * **Raymundo Márquez** *
Miguel Bernal *

* *Department of Electrical and Electronics Engineering, Sonora Institute of Technology, Ciudad Obregón, Sonora, Mexico (e-mail: raymundo.marquez@itson.edu.mx)*

Abstract: This paper presents real-time implementation results of error-based output regulation for a Twin Rotor MIMO system via a recently appeared linear matrix inequality approach, which can be solved via convex optimization techniques. Besides guaranteeing tracking of the desired trajectories provided by an exosystem, the convex formulation allows designing performance measures such as decay rate and control bounds, which are key for real-time implementation. The reported results illustrate the applicability and effectiveness of the presented approach.

Keywords: Error-Feedback Output Regulation, Twin Rotor System, Linear Matrix Inequality, Lyapunov Function.

1. INTRODUCTION

Output regulation is defined as the problem of asymptotic tracking of a reference signal under uncertainties and perturbations; the system must satisfy some stability properties in order to guarantee output regulation (Isidori, 1995). A complete solution to this problem has been provided in (Isidori and Byrnes, 1990); it is based on solving the well-known Francis-Isidori-Byrnes (FIB) equations, which arise in the field of differential geometry control techniques. Output regulation for linear (Francis, 1977; Bernal et al., 2012) and nonlinear systems (Carr, 1981; Isidori and Byrnes, 1990; Bernal et al., 2012) have been addressed in the literature. On the other hand, two regulation problems can be found: 1) State-Feedback Output Regulation Problem (SFORP), which corresponds to a situation where all states are available, and 2) Error-Feedback Output Regulation Problem (EFORP), where only the output of the system is available and, therefore, the error function.

Solving the FIB equations is a cumbersome task in the nonlinear case. This is the reason why several approaches have appeared in the recent years to tackle this problem by reducing it to a linear one via fuzzy techniques Meda and Castillo (2009) or dynamic implementation Meda et al. (2012) of the nonlinear mappings. In Bernal et al. (2012); Bernal et al. (2012) it has been proved that linear matrix inequalities (LMIs) can be used for solving the FIB equations. LMIs are highly appreciated as they allow optimal and systematic computation of solutions (Boyd et al., 1994); common control tasks such as input/output saturation limits, decay rate, and H_∞ control can be easily specified as LMIs (Duan and Yu, 2013). This paper follows the latter path by using the plant linearization as basis for LMI-based output regulation design; since real-time implementation obliges to use only those states that are available, error-feedback will be employed.

The solution obtained with the aforementioned methodology will be applied on a Twin Rotor MIMO system (TRMS), which captures the most important features of an helicopter; the main differences being that the TRMS is fixed on a pole and the position and velocity are regulated through the rotors whilst in an helicopter there is no pole and rotor velocity is almost constant, the propulsion being dependent on the angle variation of the rotor helixes (Feedback, 1998). A 9 state model will be employed in order to include the effect of the crossed couplings between the two actuators and the elevation and azimuth angles.

The main contribution of this work is a single step algorithm via linear matrix inequalities which may includes designing performance measures, an important feature in real-time implementation, such that regulation mappings as well as the control gains can be directly obtained for the EFORP. This paper is organized as follows. Section 2 describes the TRMS as well as its nonlinear model; a linearization of the latter is obtained for further developments. Section 3 provides conditions for an LMI solution of the EFORP with guaranteed decay rate. Section 4 gives the simulation and real-time implementation results of the proposed scheme when applied to the TRMS; real-time implementation issues under perturbations are also discussed. Finally, Section 5 briefs the paper results and provides some tracks for future work on the subject.

⋆ This work has been supported by the Mexican Council of Science and Technology (CONACYT) through scholarship No. 785410 and No. 791935, the Mexican Agency PRODEP via Project No. DSA/103.5/16/10200, and the Sonora Institute of Technology (ITSON) via PROFAPI Projects No. 2017_0019 and 2017_0088, Project PFCE-2016. The authors gratefully acknowledge the support of these institutions.

2. THE TWIN ROTOR

The TRMS consists on a beam fixed to a pole, as can be seen in the figure 1, with the beam having two DC motors (rotors) placed at its extremes to counterbalance gravity (Feedback, 1998). Figure 1 shows the elevation and azimuth angles labelled as x_2 and x_5, respectively. The TRMS integrates an electrical unit which transfers measured signals from encoder sensors to the PC and provides control signals to the motors through an I/O card. This unit uses a PCI I/O card model $33-007$ of Feedback Instruments and operates via MATLAB/SIMULINK. Real-time implementation of control algorithms will be performed using this platform.

There exist different models of the TRMS: a 6-state version is presented in (Tao et al., 2010; Nejjari et al., 2011), which disregards the coupling between rotors; a 7-state representation can be found in (Feedback, 1998; Ahmed et al., 2009; Gonzalez et al., 2012), which includes the internal coupling as an additional state. In this work, more information about the dynamics of the system has been considered with a 9-state model which adds the integrals of the elevation and azimuth angles. In the TRMS model (1) below, the states x_1, x_2, x_3, x_4, x_5, x_6, x_7, x_8, and x_9 correspond to the elevation motor velocity, the elevation angle, the elevation angular velocity, the tail motor velocity, the azimuth angle, the azimuth angular velocity, a coupling internal state, the elevation angle integral, and the azimuth angle integral, respectively. The elevation angle x_2 and the azimuth angle x_5 are available because they are measured with the encoder sensors; they represent the outputs of the system:

$$\begin{bmatrix}\dot{x}_1\\ \dot{x}_2\\ \dot{x}_3\\ \dot{x}_4\\ \dot{x}_5\\ \dot{x}_6\\ \dot{x}_7\\ \dot{x}_8\\ \dot{x}_9\end{bmatrix} = \underbrace{\begin{bmatrix} -0.8333 & 0 & 0 & 0 & 0 & 0 & 0 & 0 & 0\\ 0 & 0 & 1 & 0 & 0 & 0 & 0 & 0 & 0\\ E_1 & E_2 & -\dfrac{B_{1\Psi}}{I_1} & 0 & 0 & E_3 & 0 & 0 & 0\\ 0 & 0 & 0 & -1 & 0 & 0 & 0 & 0 & 0\\ 0 & 0 & 0 & 0 & -1 & 0 & 0 & 0 & 0\\ 0 & 0 & 0 & E_4 & 0 & -\dfrac{B_{1\Phi}}{I_2} & -\dfrac{1}{I_2} & 0 & 0\\ E_5 & 0 & 0 & 0 & 0 & 0 & -\dfrac{1}{I_2} & 0 & 0\\ 0 & 1 & 0 & 0 & 0 & 0 & 0 & 0 & 0\\ 0 & 0 & 0 & 0 & 1 & 0 & 0 & 0 & 0 \end{bmatrix}}_{A(x(t))} \begin{bmatrix}x_1\\ x_2\\ x_3\\ x_4\\ x_5\\ x_6\\ x_7\\ x_8\\ x_9\end{bmatrix} + \underbrace{\begin{bmatrix} 0.9166 & 0\\ 0 & 0\\ 0 & 0\\ 0 & 0.8\\ 0 & 0\\ 0 & 0\\ E_6 & 0\\ 0 & 0\\ 0 & 0 \end{bmatrix}}_{B(x(t))} \begin{bmatrix}u_1\\ u_2\end{bmatrix} \tag{1}$$

with $E_1 = \frac{b_1+a_1x_1}{I_1}\left(1 - K_{gy}x_6\cos x_2\right)$, $E_2 = \frac{-M_{fg}\sin x_2}{I_1 x_2}$, $E_3 = \frac{0.0163}{I_2}x_6\sin(2x_2)$, $E_4 = \frac{b_2+a_2x_4}{I_2}$, $E_5 = \frac{\tilde{B}(b_1+a_1x_1)}{2} - \tilde{A}\left(0.5b_1 + a_1x_1\right)$, $E_6 = 0.9166\tilde{A}\left(0.5b_1 + a_1x_1\right)$, where $I_1 = 0.068$ kg·m^2 is the moment of inertia of vertical rotor, $I_2 = 0.02$ kg·m^2 is the moment of inertia of horizontal rotor, $a_1 = 0.0135$, $b_1 = 0.0924$, $a_2 = 0.02$, and $b_2 = 0.09$ are the static characteristic parameters,

Fig. 1. Twin Rotor MIMO System

$M_{fg} = 0.32$ N·m is the gravity momentum, $B_{1\psi} = 0.006$ N·m·s/rad and $B_{1\phi} = 0.1$ N·m·s/rad are the friction momentum function parameters, $K_{gy} = 0.05$ s/rad is the gyroscopic momentum parameter, $\tilde{A} = -0.7$ and $\tilde{B} = -0.2$ are auxiliar constants.

Now, in order to apply the methodology related to output regulation, a linearization of nonlinear system (1) is necessary. The following linear state-space representation is obtained:

$$\dot{x}(t) = Ax(t) + Bu(t), \quad y(t) = Cx(t), \tag{2}$$

$$A = \left.\frac{\partial A(x)}{\partial x}\right|_{x=0} = \begin{bmatrix} -0.8 & 0 & 0 & 0 & 0 & 0 & 0 & 0 & 0\\ 0 & 0 & 1 & 0 & 0 & 0 & 0 & 0 & 0\\ 1.4 & -4.7 & 0 & 0 & 0 & 0 & 0 & 0 & 0\\ 0 & 0 & 0 & -1 & 0 & 0 & 0 & 0 & 0\\ 0 & 0 & 0 & 0 & 0 & 1 & 0 & 0 & 0\\ 0 & 0 & 0 & 4.5 & 0 & -5 & -50 & 0 & 0\\ 0 & 0 & 0 & 0 & 0 & 0 & -0.5 & 0 & 0\\ 0 & 1 & 0 & 0 & 0 & 0 & 0 & 0 & 0\\ 0 & 0 & 0 & 0 & 1 & 0 & 0 & 0 & 0 \end{bmatrix},$$

$$B = \left.\frac{\partial B(x)}{\partial x}\right|_{x=0} = \begin{bmatrix} 0.9167 & 0\\ 0 & 0\\ 0 & 0\\ 0 & 0.8\\ 0 & 0\\ 0 & 0\\ -0.0296 & 0\\ 0 & 0\\ 0 & 0 \end{bmatrix}, C = \begin{bmatrix} 0 & 1 & 0 & 0 & 0 & 0 & 0 & 0 & 0\\ 0 & 0 & 0 & 0 & 1 & 0 & 0 & 0 & 0 \end{bmatrix}.$$

Before going further, the following notations are introduced: " $<$" and " $>$" stand for matrix negative and positive definiteness, respectively; " $\prec$" and " $\succ$" stand for element-wise ordinary lower-than and greater-than relationships amongst elements of matrix expressions, respectively.

3. CONTROLLER DESIGN VIA LMIS

This section presents developments which lead to conditions in an LMI form such that the output regulation is guaranteed. It is mainly based on the works in Bernal et al. (2012); Bernal et al. (2012). Consider the following linear system:

$$\dot{x}(t) = Ax(t) + Bu(t), \quad y(t) = Cx(t), \tag{3}$$

$$\dot{w}(t) = Sw(t), \tag{4}$$

$$e(t) = Cx(t) + Qw(t), \tag{5}$$

where $x(t) \in X \subset \mathbb{R}^n$ is the state vector, $u(t) \in \mathbb{R}^m$ is the control input, $y(t) \in \mathbb{R}^o$ is the output vector, $w(t) \in W \subset \mathbb{R}^q$ is the state vector of an exosystem, $e(t) \in \mathbb{R}^o$ is the error vector, $A \in \mathbb{R}^{n\times n}$, $B \in \mathbb{R}^{n\times m}$, $S \in \mathbb{R}^{q\times q}$, $C \in \mathbb{R}^{o\times n}$, and $Q \in \mathbb{R}^{o\times q}$ are known matrices.

The dynamic system in (4) is called exosystem which generates the reference signals to be tracked. Exosystem is assumed to be neutral stable, which means that all the eigenvalues of matrix S are in the imaginary axes in the complex plane leading to periodic orbits. The best scenario, from a "feedback point of view", happens when all states are accessible. However, recall that for the TRMS not all of them are available (only x_2 and x_5 of 9 states), which is why we turn to an error-feedback scheme.

The Linear Error-Feedback Output Regulation Problem (LEFORP) consists on finding a control law based on a error-feedback dynamic observer with the following structure:

$$\begin{aligned} \dot{\xi}(t) &= F\xi(t) + Ge(t), \\ u(t) &= H\xi(t), \end{aligned} \tag{6}$$

where $\xi(t) = \left[\xi_f^T(t)\ \xi_s^T(t)\right]^T \in \Xi \subset \mathbb{R}^{n+q}$, $\xi_f(t) \in \mathbb{R}^n$ goes to $x(t)$ when $t \to \infty$, $\xi_s(t) \in \mathbb{R}^q$ goes to $w(t)$ when $t \to \infty$.

The design matrices $F \in \mathbb{R}^{(n+q)\times(n+q)}$, $G = \left[G_0^T\ G_1^T\right]^T$, $G_0 \in \mathbb{R}^{n\times m}$, $G_1 \in \mathbb{R}^{q\times m}$, and $H \in \mathbb{R}^{m\times(n+q)}$ must guarantee that $\forall(x(0), \xi(0), w(0)) \in \Omega \subset X \times \Xi \times W$, the error (5) is driven to zero and the extended matrix

$$\begin{bmatrix} A & BH \\ GC & F \end{bmatrix} \tag{7}$$

is Hurwitz, thus, the control input $u(t)$ stabilizes the linear system (3) when $w(t) = 0$.

The LEFORP has solution if and only if (Francis, 1977):

(1) $\mathrm{Re}\{\sigma(S)\} \geq 0$, the pair (A, B) is stabilizable, and the pair $\left(\begin{bmatrix} A & 0 \\ 0 & S \end{bmatrix}, [C\ Q]\right)$ is detectable.
(2) $\exists\Pi \in \mathbb{R}^{n\times q}$, $\exists\Gamma \in \mathbb{R}^{m\times q}$ such that (8) and (9) holds.

$$\Pi S = A\Pi + B\Gamma, \tag{8}$$
$$0 = C\Pi + Q. \tag{9}$$

The procedure to solve the LEFORP is described hereafter:

(1) Find a matrix K such as $(A + BK)$ is Hurwitz.
(2) Search matrices Π and Γ such as (8) and (9) are satisfied.
(3) Find a matrix $G = \begin{bmatrix} G_0 \\ G_1 \end{bmatrix}$ such as

$$\left(\begin{bmatrix} A & 0 \\ 0 & S \end{bmatrix} - \begin{bmatrix} G_0 \\ G_1 \end{bmatrix} [C\ Q]\right) \tag{10}$$

is Hurwitz. Then, the matrices F and H in the dynamic observer (6) can be constructed as follows:

$$F = \begin{bmatrix} A + BK - G_0C & B\,(\Gamma - K\Pi) - G_0Q \\ -G_1C & S - G_1Q \end{bmatrix}, \tag{11}$$
$$H = [K\ \Gamma - K\Pi]\,. \tag{12}$$

(4) Apply control law $u(t) = H\xi(t)$ to system (3).

The aforementioned steps can be performed in a systematic way via LMIs. In order to get the gain matrix K, consider a linear system as in (2) with a linear state-feedback $u = Kx$. The direct Lyapunov method is applied to find the controller gain K. Let consider a quadratic Lyapunov function $V(x) = x^T P_1 x$, $P_1 = P_1^T > 0$. The closed-loop system $\dot{x} = (A + BK)x$ is stable with decay-rate $\alpha_1 > 0$ if and only if $\dot{V}(x) + \alpha_1 V(x) < 0$. Then, LMIs conditions such that these performances hold are:

$$AX_1 + BM_1 + X_1A^T + M_1^TB^T + 2\alpha_1X_1 < 0, X_1 > 0, \tag{13}$$

where $X_1 = X_1^T \in \mathbb{R}^{n\times n}$ and $M_1 \in \mathbb{R}^{m\times n}$. Once, LMIs (13) are solved for decision variables X_1 and M_1, the Lyapunov matrix P_1 and matrix K are computed with $P_1 = X_1^{-1}$ and $K = M_1X_1^{-1}$, respectively.

Using a similar path with $V(\xi) = \xi^T P_2 \xi$, $P_2 = P_2^T > 0$ and decay-rate $\alpha_2 > 0$, the matrix G such that (10) is Hurwitz can be found solving the following LMI conditions:

$$P_2\bar{A} - L\bar{C} + \bar{A}^TP_2 - \bar{C}^TL + 2\alpha_2P_2 < 0, P_2 > 0 \tag{14}$$

where $\bar{A} = \begin{bmatrix} A & 0 \\ 0 & S \end{bmatrix}^T$, $\bar{C} = [C\ Q]$, $P_2 \in \mathbb{R}^{(n+q)\times(n+q)}$, and $L \in \mathbb{R}^{(n+q)\times m}$. Then, the observer gains G is computed as $G = P_2^{-1}L$.

An algorithm to find mappings Π and Γ based on element-wise LMIs has been presented in (Bernal et al., 2012). It consists on approximating the solution of the matrix equalities (8) and (9) with arbitrarily small accuracy by the following element-wise LMI minimization problem:

$$\min \varepsilon > 0 : -\varepsilon \prec \begin{bmatrix} A\Pi + B\Gamma - \Pi S & 0 \\ 0 & C\Pi + Q \end{bmatrix} \prec \varepsilon. \tag{15}$$

Important features of this methodology is the fact that all set of LMIs to solve the LEFORP can be run simultaneously in a one-step algorithm as well as the possibility of including easily design performances as decay-rate or input saturation limits.

4. SIMULATION AND REAL-TIME RESULTS

In this section, simulation and real-time results on TRMS are provided to illustrate the applicability and effectiveness of the approach. Algorithms have been programmed using LMI toolbox (Gahinet et al., 1995) within a MATLAB R2009b platform. Simulations as well as real-time implementations have been performed using the files developed by Feedback Instruments and a PCI I/O card model $33-007$ which operates via Simulink/MATLAB (Feedback, 1998).

Using a one-step LMI-based algorithm, it includes conditions (13), (14), and (15), the Error-Feedback Output regulation Problem has been solved for the Twin Rotor MIMO System. Considering matrices $S = \begin{bmatrix} 0 & 1 \\ -1 & 0 \end{bmatrix}$ and $Q = \begin{bmatrix} -1 & 0 \\ 0 & -1 \end{bmatrix}$ and parameters $\alpha_1 = 0.5$ and $\alpha_2 = 0$, the matrices K, G, F as well as mapping matrices Π and Γ obtained with $\varepsilon = 1.0432 \times 10^{-14}$ are:

$$K = \begin{bmatrix} -5.2972 & -4.3621 & -10.451 & 7.4775 & 3.2884 & \cdots \\ -4.7731 & -10.927 & -9.4577 & 0.64519 & -19.946 & \cdots \\ \cdots & -6.2104 & -75.925 & -16.131 & 1.0896 & \\ \cdots & -11.798 & -2.918 & -15.344 & -11.914 & \end{bmatrix},$$

$$G = \begin{bmatrix} 197.6981 & -211.4687 \\ -194.2871 & 51.9891 \\ -172.8943 & 284.9827 \\ -377.7510 & -46.4687 \\ -460.2259 & 393.8069 \\ 148.8703 & 137.9026 \\ -50.5104 & -17.8182 \\ 40.8125 & -42.4657 \\ -223.3986 & 57.0063 \\ -223.3986 & 56.0063 \\ -456.6317 & 368.1400 \end{bmatrix},$$

$$F = \begin{bmatrix} -5.68 & -201.69 & -9.58 & 6.85 & 214.48 & \cdots \\ 0 & 194.28 & 1 & 0 & -51.98 & \cdots \\ 1.35 & 168.18 & -0.08 & 0 & -284.98 & \cdots \\ -3.81 & 369.00 & -7.56 & -0.48 & 30.51 & \cdots \\ 0 & 460.22 & 0 & 0 & -393.80 & \cdots \\ 0 & -148.87 & 0 & 4.5 & -137.90 & \cdots \\ 0.17 & 50.63 & 0.30 & -0.22 & 17.72 & \cdots \\ 0 & -39.81 & 0 & 0 & 42.46 & \cdots \\ 0 & 223.39 & 0 & 0 & -56 & \cdots \\ 0 & 223.39 & 0 & 0 & -56 & \cdots \\ 0 & 456.63 & 0 & 0 & -368.14 & \cdots \end{bmatrix}$$

$$\begin{bmatrix} \cdots & -5.69 & -69.6 & -14.78 & 0.99 & 218.59 & -214.95 \\ \cdots & 0 & 0 & 0 & 0 & -194.28 & 51.98 \\ \cdots & 0 & 0 & 0 & 0 & -172.89 & 284.98 \\ \cdots & -9.43 & -2.33 & -12.27 & -9.53 & -359.24 & -37.21 \\ \cdots & 1 & 0 & 0 & 0 & -460.22 & 393.80 \\ \cdots & -5 & -50 & 0 & 0 & 148.87 & 137.90 \\ \cdots & 0.18 & 1.74 & 0.47 & -0.03 & -51.18 & -17.70 \\ \cdots & 0 & 0 & 0 & 0 & 40.81 & -42.46 \\ \cdots & 0 & 0 & 0 & 0 & -223.39 & 57 \\ \cdots & 0 & 0 & 0 & 0 & -223.39 & 57 \\ \cdots & 0 & 0 & 0 & 0 & -457.63 & 368.14 \end{bmatrix},$$

$$\Pi = \begin{bmatrix} 2.7273 & 0.0649 \\ 1 & 0 \\ 0 & 1 \\ -2.0015 & -0.4117 \\ 0 & 1 \\ -1 & 0 \\ -0.0801 & -0.0171 \\ 0 & -1 \\ 1 & 0 \end{bmatrix}, \Gamma = \begin{bmatrix} 2.4084 & 3.0342 \\ -1.9873 & -3.0165 \end{bmatrix}.$$

The controller gain H in (12) is:

$$H = \begin{bmatrix} -5.297 & -4.362 & -10.451 & 7.478 & 3.288 & \cdots \\ -4.773 & -10.927 & -9.458 & 0.645 & -19.946 & \cdots \\ \cdots & -6.21 & -75.93 & -16.13 & 1.09 & 22.8 & -3.81 \\ \cdots & -11.8 & -2.92 & -15.34 & -11.91 & 23.13 & 11.57 \end{bmatrix}$$

Observe that due to the definition of S, the exosystem (4) provides sinusoidal references for w_1 and w_2. As stated before, the main objective is that $x_2 \to w_1$ and $x_5 \to w_2$ as $t \to \infty$. The control input (6) based on an error-feedback dynamics observer has been applied to the original model (1) of TRMS using the provider files for simulation, it shades some light about real-time implementation, for instance, concerning the range of control signals.

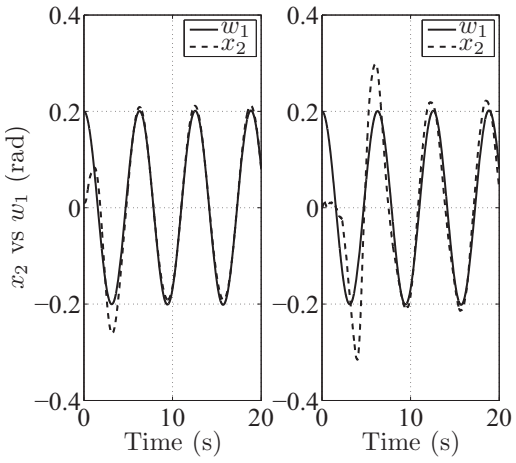

Fig. 2. Elevation angle: simulation (left), real-time (right)

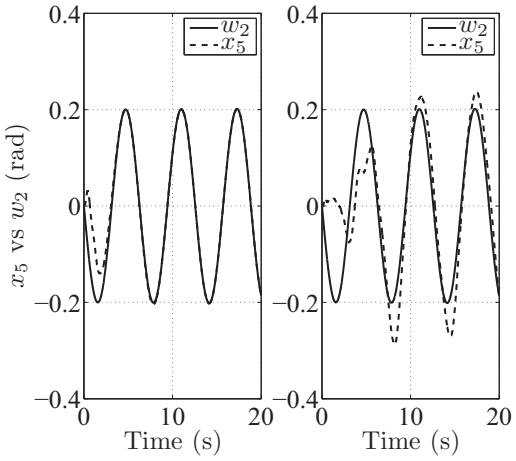

Fig. 3. Azimuth angle: simulation (left), real-time (right)

Despite simulation performing adequately, sometimes real-time does not: it may lack energy on the actuators, surpass their saturation limits, or being unable to deal with unmodelled dynamics. Figures 2, 3, and 4 show the time-response behavior of x_2 (elevation angle), x_5 (azimuth angle), and control law u, both simulation (left) and real-time (right). The initial conditions are $x(0) = \xi_f(0) = 0 \in \mathbb{R}^n$ and $w(0) = \xi_s(0) = [0.2\ 0]^T$.

Simulation results are very similar to those in real-time. The elevation angle (x_2) and the azimuth angle (x_5) need less time in simulation than real-time to follow the reference signals w_1 and w_2, respectively; see figures 2 and 3. The approximation nature of the employed linear scheme as well as noisy signals during implementation are accountable for higher errors in real-

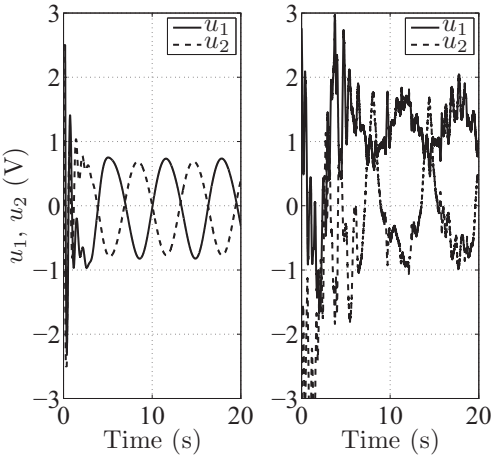

Fig. 4. Control input: simulation (left), real-time (right)

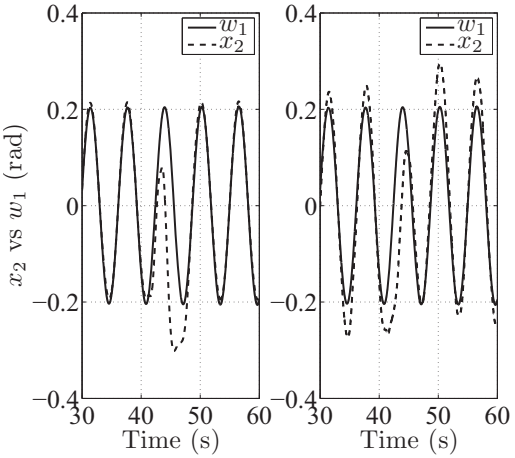

Fig. 5. Elevation angle (disturbed): simulation (left), real-time (right)

time than simulation; this can be better appreciated comparing the control signals (see figure 4). The actuator limits for inputs in the TRMS are ± 2.5 volts; since these limits are satisfied when the controller is implemented, it is not necessary to consider them for LMI additional conditions.

Also, a systematic vanished perturbation has been applied to test the regulation scheme performance. It consists on adding -2 volts from the second 41 to 43 to control signals u_1 and u_2. In this case, we use a gain K_2 with decay rate $\alpha_1 = 2.7$. The results for x_2 and x_5 are shown in figures 5 and 6. As expected, the elevation angle x_2 has more difficulty than the azimuth angle x_5 to follow the reference signal after the perturbation is applied. In figure 7 it is possible to appreciate the effect of the perturbation at second $t = 41$.

$$K_2 = \begin{bmatrix} 17181 & -1108.8 & -3081.7 & 2.762 & 7.9341 & \cdots \\ 216.74 & 60.156 & -1.1068 & -14.172 & -297.53 & \cdots \\ \cdots & -0.48359 & 533080 & -20336 & 4.3552 & \\ \cdots & -43.629 & 6687.7 & -202.1 & -516.7 & \end{bmatrix},$$

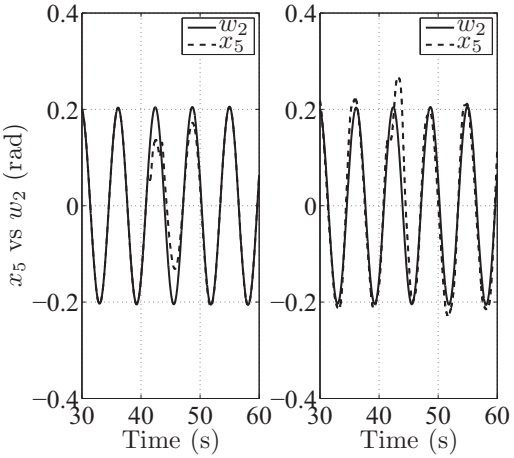

Fig. 6. Azimuth angle (disturbed): simulation (left), real-time (right)

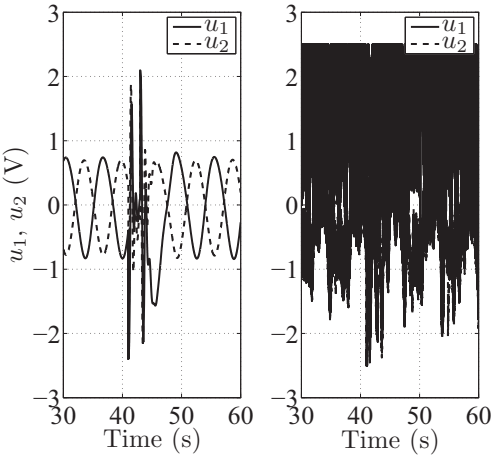

Fig. 7. Control input (disturbed): simulation (left), real-time (right)

5. CONCLUSIONS

The Error-Feedback Output Regulation Problem has been addressed through convex optimization techniques. Through a highly nonlinear plant as the Twin Rotor MIMO system, it has been shown that an error-based structure can be applied when only partial information (outputs) of the system are available. The control gains and regulation mappings have been obtained in a single step via a linear matrix inequality algorithm, which guarantees convergence of the outputs to the signal references provided by the exosystem. Simulation and real-time results have been provided to illustrate the applicability and effectiveness of the approach. As future work, a nonlinear approach via LMIs which expectedly will take into account the nonlinearities hereby neglected, is worth exploring, as trajectory tracking may improve.

REFERENCES

Ahmed, Q., Bhatti, A.I., and Iqbal, S. (2009). Robust decoupling control design for twin rotor system using

hadamard weights. In *Control Applications,(CCA) & Intelligent Control,(ISIC), 2009 IEEE*, 1009–1014. IEEE.

Bernal, M., Marquez, R., Estrada, V., and Castillo, B. (2012). An element-wise linear matrix inequality approach for output regulation problems. In *World Automation Congress (WAC), 2012*, 1–6. Puerto Vallarta.

Bernal, M., Marquez, R., Estrada-Manzo, V., and Castillo-Toledo, B. (2012). Nonlinear output regulation via Takagi-Sugeno fuzzy mappings: A full-information LMI approach. In *Fuzzy Systems (FUZZ-IEEE), 2012 IEEE International Conference on*, 1–7. IEEE.

Boyd, S., Ghaoui, L.E., Feron, E., and Belakrishnan, V. (1994). *Linear Matrix Inequalities in System and Control Theory*, volume 15. SIAM: Studies In Applied Mathematics, Philadelphia, USA.

Carr, J. (1981). Applications of center manifold theory springer-verlag: Newyork. *Heidelberg, Berlin*.

Duan, G. and Yu, H. (2013). *LMIs in Control Systems: Analysis, Design and Applications*. CRC Press, Boca Raton, Florida.

Feedback (1998). *TRMS 33-949S User Manual: Twin Rotor MIMO System Control Experiments*. Feedback instruments Ltd, East Sussex, U.K.

Francis, B. (1977). The linear multivariable regulator problem. *SIAM Journal of Control and Optimization*, 15, 486–505.

Gahinet, P., Nemirovski, A., Laub, A.J., and Chilali, M. (1995). *LMI Control Toolbox*. Math Works, Natick, USA.

Gonzalez, T., Rivera, P., and Bernal, M. (2012). Nonlinear control for plants with partial information via Takagi-Sugeno models: An application on the twin rotor MIMO system. In *2012 9th International Conference on Electrical Engineering, Computing Science and Automatic Control (CCE)*, 7–12.

Isidori, A. (1995). *Nonlinear Control Systems*. Springer, London, 3 edition.

Isidori, A. and Byrnes, C.I. (1990). Output regulation of nonlinear systems. *IEEE Transactions on Automatic Control*, 35(2), 131–140.

Meda, J.A. and Castillo, B. (2009). Synchronization of chaotic systems from a fuzzy regulation approach. *Fuzzy Sets and Systems*, 160(19), 2860–2875.

Meda, J.A., Gomez, J.C., and Castillo, B. (2012). Exact output regulation for nonlinear systems described by Takagi-Sugeno fuzzy models. *IEEE Transactions on Fuzzy Systems*, 20(2), 235–247.

Nejjari, F., Rotondo, D., Puig, V., and Innocenti, M. (2011). Lpv modelling and control of a twin rotor mimo system. In *Control & Automation (MED), 2011 19th Mediterranean Conference on*, 1082–1087. IEEE.

Tao, C.W., Taur, J.S., Chang, Y.H., and Chang, C.W. (2010). A novel fuzzy-sliding and fuzzy-integral-sliding controller for the twin-rotor multi-input–multi-output system. *IEEE transactions on Fuzzy Systems*, 18(5), 893–905.